Detection of microbial disturbances in a drinking water microbial community through continuous acquisition and advanced analysis of flow cytometry data

Ruben Props[a], Peter Rubbens[b], Michael Besmer[c,d], Benjamin Buysschaert[a], Jurg Sigrist[c], Hansueli Weilenmann[c], Willem Waegeman[b], Nico Boon[a] and Frederik Hammes[c,*]

[a] Center for Microbial Ecology and Technology (CMET), Ghent University, Coupure Links 653, B-9000 Gent, Belgium

[b] KERMIT, Department of Data Analysis and Mathematical Modelling, Ghent University, B-9000 Ghent, Belgium

[c] Eawag, Swiss Federal Institute of Aquatic Science and Technology, Ueberlandstrasse 133, CH-8600 Duebendorf, Switzerland

[d] Department of Environmental Systems Science, Institute of Biogeochemistry and Pollutant Dynamics, ETH Zürich, Zürich, Switzerland

* **Corresponding author:**

Name: Frederik Hammes

Tel.: +41 58 765 5372

Email: frederik.hammes@eawag.ch

This document is the accepted manuscript version of the following article:
Props, R., Rubbens, P., Besmer, M., Buysschaert, B., Sigrist, J., Weilenmann, H., … Hammes, F. (2018). Detection of microbial disturbances in a drinking water microbial community through continuous acquisition and advanced analysis of flow cytometry data. Water Research, 145, 73-82. https://doi.org/10.1016/j.watres.2018.08.013

Abstract

Detecting disturbances in microbial communities is an important aspect of managing natural and engineered microbial communities. Here, we implemented a custom-built continuous staining device in combination with real-time flow cytometry (RT-FCM) data acquisition, which, combined with advanced FCM fingerprinting methods, presents a powerful new approach to track and quantify disturbances in aquatic microbial communities. Through this new approach we were able to resolve various natural community and single-species microbial contaminations in a flow-through drinking water reactor. Next to conventional FCM metrics, we applied metrics from a recently developed fingerprinting technique in order to gain additional insight into the microbial dynamics during these contamination events. Importantly, we found that multiple community FCM metrics based on different statistical approaches were required to fully characterize all contaminations. Furthermore we found that for accurate cell concentration measurements and accurate inference from the FCM metrics (coefficient of variation ≤ 5%), at least 1,000 cells should be measured, which makes the achievable temporal resolution a function of the prevalent bacterial concentration in the system-of-interest. The integrated RT-FCM acquisition and analysis approach presented herein provides a considerable improvement in the temporal resolution by which microbial disturbances can be observed and simultaneously provides a multi-faceted toolset to characterize such disturbances.

Keywords: flow cytometry, disturbance ecology, drinking water, fingerprinting, microbial ecology

1. Introduction

Monitoring and managing microbial and physicochemical dynamics within engineered aquatic systems (e.g., drinking and cooling water systems, wastewater treatment) is an important research area in environmental engineering (Verstraete et al. 2007). Such dynamics can transpire within minutes (Koch et al. 2014), hours (Lautenschlager et al. 2010, Props et al. 2016a) or days (Guenther et al. 2012, Besmer et al. 2016). In particular in engineered aquatic systems, ecological disturbances are either present continuously through spatially separated treatment steps (e.g., ozonation, UV-disinfection) or sporadically through uncontrolled events (e.g., weather events (Zhang et al. 2017), contamination (Besmer and Hammes 2016), outgrowth (Props et al. 2016b)). The assessment of these rapid microbial processes through sampling at discrete time points is prone to so-called 'aliasing', i.e. bias in the observed frequency and/or the kinetics of the events, which can have considerable impacts on public health and product quality.

As a result, the development of high-frequency monitoring techniques for detecting microbial community disturbances has gained momentum. Flow cytometry (FCM) is a multi-purpose single-cell analysis tool for studying microorganisms. Conventional *manual FCM* entails the collection of homogeneous samples, which are subsequently stained and measured by the operator. The transition from manual operation towards automation started with hardware developments in phytoplankton research aimed at the direct detection of cell size and auto-fluorescence (Dubelaar et al. 1999, Dubelaar and Gerritzen 2000). Recently, so-called *online FCM* has allowed the complete automation of the measurement process; discrete samples are automatically collected, stained, incubated and analyzed at routine intervals (typically 5 – 15 minutes) during extended time periods (days - months) (Besmer et al. 2014, Hammes et al. 2012, Abu-Absi et al. 2003, Zhao et al. 1999).

A potential paradigm shift in FCM operation and analysis is so-called kinetic or *real-time* flow cytometry (RT-FCM), which exploits the inherent time-dependent nature of any FCM analysis (Martin and Swartzendruber 1980, Nolan and Sklar 1998, Arnoldini et al. 2013). In its most basic form, RT-FCM simply records single-cell data as a function of measuring time, which is a feature available on most commercial instruments (Arnoldini et al. 2013). In this context, RT-FCM has been applied to experiments where fluorescent staining is not required (e.g., green fluorescent protein (GFP) expression), or where a combination

of the stain and the immediate experimental environment is specifically required (e.g., assessment of stain-cell interactions) (Arnoldini et al. 2013, Vines et al. 2010, Juan et al. 1994). However, fluorescent labelling of the target cells is required for all studies characterizing indigenous microbial communities as they are otherwise not detectable. Two recent studies have described the first applications of RT-FCM data in combination with purpose-build automated staining devices (Besmer and Hammes 2016, Besmer et al. 2017).

FCM applications range from straightforward cell density measurements to complicated phenotypic assays such as cellular type, identity, viability and physiology (Shapiro 1983, Hammes and Egli 2010, Muller 2007, Mueller and Nebe-von-Caron 2010, Berney et al. 2008). Up till now, FCM data has been primarily used to describe the microbial dynamics by means of descriptive metrics such as total cell density, intact cell density as well as a basic FCM fingerprint statistic (e.g., % high nucleic acid (HNA) content bacteria) (Prest et al. 2013, Bouvier et al. 2007). Similar to phytoplankton FCM data (Li 1997), bacterial FCM data has recently been shown to contain a significant amount of taxonomic community structure as well (Props et al. 2016a, Rubbens et al. 2017, Stepanauskas et al. 2017, Props et al. 2018). Novel computational FCM analysis tools, such as the phenotypic diversity index, now facilitate simultaneous tracking of taxonomic diversity and cytometric community structure based solely on multivariate FCM data derived from nucleic acid stained bacterial cells (Props et al. 2016a, Koch et al. 2013a, Koch and Müller 2017, Amalfitano et al.). All of these FCM metrics rely on the stability, reproducibility and sample sizes that can be obtained from FCM measurements, yet a quantitative assessment on the sample sizes, which may vary between hundreds to millions of cells, that are required for robust inference has not yet been performed.

Here we integrated real-time staining and FCM data acquisition technology with advanced fingerprinting metrics (i.e. phenotypic diversity index and phenotypic community type) with the goal of detecting and characterizing microbial disturbances in a drinking water microbial community at the highest possible temporal resolution. The goals of this study were: (1) to demonstrate that advanced data analysis (i.e. fingerprinting) techniques are necessary to characterize simple and complex microbial disturbances in real-time FCM data, and (2) to systematically assesses the acquisition requirements (e.g., sample size) in order to maximize the temporal resolution for microbial community fingerprint metrics.

2. Materials and Methods

2.1. Real-time flow cytometry

We applied a previously described prototype system that continuously extracts, stains and incubates water samples from any experimental environment and loads these continuously onto a commercially available flow cytometer for analysis (Besmer et al. 2017). The prototype extracts samples continuously with peristaltic pumping at a rate of 0.3 mL min^{-1} and then stains these samples continuously in a mixing chamber with a fluorescent dye, also at a rate of 0.3 mL min^{-1}. In this study we used SYBR Green I (Invitrogen), diluted 5,000-fold in TRIS-buffer. The result is a 50 % final dilution of both the sample and dye at a combined flow rate of 0.6 mL min^{-1}. From the mixing chamber the stained sample flows through an incubation loop (0.75 mm PEEK tubing) at a controlled temperature (37 °C). A pre-calculated loop length dictates the incubation time (10 minutes), after which the sample is delivered to a purpose-built sampling port compatible with a commercially available flow cytometer (Accuri C6; Becton Dickinson Biosciences, Erembodegem, Belgium). The FCM was equipped with a 488 nm laser with detectors for green fluorescence (533±30 nm) and deep red fluorescence (>670 nm), as well as for forward scatter (FSC) and sideward scatter (SSC) light. Data were collected continuously using the instrument's "unlimited run" function as described previously (Arnoldini et al. 2013), with the sampling speed programmed on 16 μL min^{-1} at data acquisition rates varying between 50 – 1,000 events $second^{-1}$.

2.2. Data acquisition stability

A non-chlorinated municipal drinking water sample (Dübendorf, Switzerland) was measured continuously for 60 minutes to assess the stable operation of the staining device and the overall quality of the data produced. The experiment was repeated three times. The experiment was subsequently repeated with river water (Chriesbach River; Dübendorf, Switzerland) to assess differences in data quality at high and low bacterial concentrations.

2.3. Contamination by axenic cultures

A flow-through continuous stirred reactor (60 mL) with magnetic stirring was used to test the system's performance in a dynamic environment (**Figure 1**). The reactor was continuously fed for 60 min with non-chlorinated municipal drinking water at a flow-rate of 100 mL min^{-1}, thus enabling 1.7 volume changes per minute. The feed water was kept in a 5 L reservoir and remained unchanged during the experiment. After 10 minutes of baseline measurements, the drinking water was successively spiked thrice with an axenic culture of *Escherichia coli* (MG1655, ATCC 25922) and thereafter thrice with an axenic culture of *Pseudomonas stutzeri* (A1501, Pasteur Institute). The axenic cultures were grown overnight at 30 °C in LB media, centrifuged (3 min; 3,000 g) and suspended in non-chlorinated drinking water and 50 mM EDTA to a final concentration of 545 cells μL^{-1} (*E. coli*) and 524 cells μL^{-1} (*P. stutzeri*). Each individual spiking event comprised two minutes of continuous spiking using a speed-controlled syringe pump (at 1 mL min^{-1}) and eight minutes of subsequent washout (approximately 13 reactor volume changes).

2.4. Contamination by natural microbial communities

The same flow-through reactor as above was used to assess more challenging disturbances, such as those presented by natural aquatic microbial communities. After 10 minutes of baseline measurements, the feed water was changed at 10-minute intervals to respectively bottled mineral water (Evian, France), groundwater (Dübendorf, Switzerland), 20-fold diluted pond water (Dübendorf, Switzerland), 10-fold diluted river water (Chriesbach River, Dübendorf, Switzerland), 20-fold diluted river water (Glatt River, Dübendorf, Switzerland) and finally again municipal drinking water (as above). Each water sample replaced the previous during 10 minutes (equaling 25 volume changes). Prior to the experiment, the contaminant communities were diluted to cell densities in the same order of magnitude as the drinking water community in order to create subtle transitions in the microbial community that would be more challenging to detect. The data were specifically analyzed with respect to the sensitivity of the system to detect gradual changes and differentiate between complex samples.

147 **2.5. Data processing and statistical analysis**

148 Raw experimental data were collected with the FCM software (BD Accuri C6 Software). All data processing
149 steps and statistical analyses were conducted in the R statistical environment (v3.3.0, seed = 777) with the
150 *Phenoflow* package (v1.1, https://github.com/CMET-UGent/Phenoflow_package) and its dependencies.
151 Each experiment generated a single FCS file, which was denoised (**Figure S1**), discretized in user defined
152 time intervals (e.g., 10s, 30 s), and stored in separate FCS files using the *time_discretization* function. The
153 denoised and discretized data were then used to calculate the total cell concentration and high nucleic acid
154 (HNA) cell concentration using the gating and data processing strategy of Arnoldini et al. (2013). For each
155 sample a phenotypic diversity index was calculated through advanced fingerprinting of the data using the
156 *Diversity_rf* function with default settings (Props et al. 2016a). This function performs bivariate kernel density
157 estimations on selected channels (FL1-H, FL3-H, SSC-H and FSC-H), and concatenates the normalized
158 density values into a one-dimensional feature vector from which the phenotypic diversity index can be
159 calculated. There was one outlier event in the river water data set that was caused by the introduction of an air
160 bubble in the fluidics. As this event was diagnosed as a technical issue, the TCC and phenotypic diversity
161 index of this observation were replaced by the 95 % quantile value of their respective data set.

162 In addition to these continuous metrics, all samples per experiment (n) were clustered based on their
163 fingerprints by means of k-medoids clustering to create so-called phenotypic community types (Reynolds et
164 al. 2006). First, the informative features of the fingerprint were selected through principal component analysis
165 by limiting the number of principal components to those that explained 90 % of the variance. Next, k-
166 medoids clustering was performed by varying the number of clusters from 2 to n-1 (*pam* function, *cluster*
167 package (v2.0.6)). The robust number of clusters (phenotypic community types) was determined by evaluating
168 the silhouette index, and selecting k for which the average silhouette index across clusters was maximal
169 (Rousseeuw 1987). To account for differences in sample size, this workflow was repeated for 100 bootstrap
170 samples, after which the most frequent community type for each sample was determined as representative
171 cluster. The bootstrap score was calculated as the number of times that the representative community type
172 was assigned to the sample. Contrasts between the fingerprints of each cluster were calculated using the

fp_contrasts function on default settings. Longitudinal analysis of the diversity parameters and cell densities binned on 60 s intervals was performed by a model based approach. Generalized additive modelling (*mgcv* package (v1.8-12)) was performed with time as the sole fixed effect. Although there was only limited temporal autocorrelation present in the data (assessed with the *acf* function from the *stats* package (v3.3.0)), a continuous autoregressive function of order 1 was implemented. All models were checked for normal and homoscedastic residual distributions as well as autocorrelation in the residuals (Ljung-Box test). Statistical inference on the time effect was performed by the Wald's test. All figures were made using *ggplot2* (v2.2.1).

Data availability

The full data analysis workflow is publicly available at https://github.com/rprops/Real-Time_FCM. The raw flow cytometry data have been deposited on FlowRepository and are publicly available under accession ID FR-FCM-ZY5P.

3. Results

As described above, a lab-scale flow-through reactor containing a drinking water microbial community was periodically disturbed by either single-species contaminations or by complex natural microbial communities (**Figure 1**). The data acquired through real-time flow cytometric monitoring was then specifically analyzed by various conventional and fingerprinting metrics in order to characterize and differentiate between the disturbances. For this purpose we employed two conventional FCM metrics (i.e. total cell concentration (TCC), and high nucleic acid (HNA) bacteria), and two advanced fingerprinting metrics (i.e. phenotypic diversity index and phenotypic community typing). While the phenotypic diversity index has been shown to be strongly correlated to the taxonomic diversity of various aquatic microbial communities, phenotypic community typing clusters microbial community fingerprints into discrete groups or "types" with similar FCM properties.

3.1. Stability and robustness of RT-FCM data acquisition

First, the stability of the flow-through reactor and the FCM data acquisition was evaluated for drinking water and river water microbial communities over 60 minute time periods. Both microbial communities showed different degrees of stability for total cell concentration (TCC) and the phenotypic diversity index in function of the chosen temporal resolution (**Figure 2**). For the phenotypic diversity index, a clear linear relationship between the coefficient of variation (CV, relative standard deviation expressed in %) and the number of cells measured (~ temporal resolution) was found. For the TCC, a non-linear relationship was observed; the CV was ~5% for measurements which analyzed approximately 1,000 cells per sample, corresponding to a temporal resolution of one-to-two minutes for the drinking water community and 10 - 30 seconds for the river water community. We found that a lower threshold value in the range of 1,000 cells per time interval provides a good trade-off between temporal resolution and accuracy. Therefore, we adopted one-minute measurement intervals for all subsequent data analysis in this study. The average value (n = 60) for TCC was 30.1 ± 1.9 cells μL^{-1}, for %HNA content cells it was 32.6 ± 2.1%, and for the phenotypic diversity index it was 2154.6 ± 97.7 a.u.. Two additional repetitions of the same experiment with drinking water confirmed the

reproducibility of the experiment and the data analysis (**Figures S2 and S3**). The temporal trajectory of the phenotypic diversity index and total cell density could be adequately modelled by means of a generalized additive model. There was no significant temporal drift of the phenotypic diversity index over the 60 minute time period for both the tap and river water communities ($p = 0.49$). This indicates that the multivariate properties of the microbial community were accurately measured throughout the entire experiment. However, the cell densities did show a marginal ($p = 0.001$) drift over time for both the tap (average slope = 0.35 ± 0.99 cells μL^{-1} min^{-1}) and river water communities (average slope = -0.14 ± 1.05 cells μL^{-1} min^{-1}).

3.2. Detecting and differentiating between single species disturbances

As the RT-FCM data generated stable and robust metrics we challenged the drinking water microbial community with two different axenic bacterial cultures (*E. coli* and *P. stutzeri*) (**Figure 3**). The presence of these axenic cultures in the drinking water community could be easily detected visually on basic fluorescence plots, and served as a positive control for our proposed approach. The initial drinking water microbial community contained 45.6 ± 3.3 cells μL^{-1} with 37.7 ± 1.7 % HNA cells and a phenotypic diversity index of approximately 2246.3 ± 99.9 a.u. During spiking, the cell concentrations reached maxima of 207.9 cells μL^{-1} (*E. coli*) and 180.6 cells μL^{-1} (*P. stutzeri*) (Figure 3A). The % HNA content cells increased to 87.3 % during *E. coli* contamination and to 80.3 % during *P. stutzeri* contamination (Figure 3B) while concurrently the phenotypic diversity index decreased to a minimum of 977.8 a.u. and 1338.6 a.u., respectively (Figure 3C)). Clustering of the phenotypic fingerprints resulted in the identification of three distinct phenotypic community types throughout the experiment (**Figure 3D**). These represent sample groups of similar phenotypic fingerprints, and reveal changes in the community structure as a result of the contaminations. Community type 1 represented the natural drinking water community, community type 2 the *E. coli* contaminated community, and community type 3 the *P. stutzeri* contaminated community. Three data points situated at the transitions between community types had bootstrap confidence values less than 90 and thus could not be unequivocally assigned to a single community type. The combined use of FCM metrics demonstrated that it is

possible to detect both sudden (spiking) and gradual (washout) fluctuations at high temporal resolution and to discriminate between the water matrix and the different axenic cultures.

3.3. Detecting and differentiating between complex microbial community disturbances

Next, the sampling system and subsequent data analysis was challenged to detect transitions between contaminations of five different natural freshwater microbial communities (see section 2.4.). These were retrieved from grab samples of two distinct rivers, one freshwater pond, one groundwater reservoir, and a commercial bottled water. Freshwater communities from such systems have previously been shown to differ greatly in terms of their flow cytometric properties and community composition, often as a result of environmental factors (e.g., rain events, nutrient status, contamination) (Besmer et al. 2016, Prest et al. 2013, De Roy et al. 2012, Proctor et al. 2018). As such, these different freshwater systems form an ideal set of diverse communities by which our integrated RT-FCM approach can be challenged.

Only by using a combination of both conventional (TCC and % HNA cells) and advanced FCM metrics (phenotypic diversity index and phenotypic community typing) was it possible to detect and discriminate between all five contaminations, while this was not possible with any single metric (**Figure 4**). Based on observations that exceeded > 2 standard deviations from the reference mean (first 15 minutes of experiment), two major community transitions could be detected through the cell density dynamics (i.e., 30 minute and 60 minute mark, **Figure 4A**) and one additional disturbance could be detected through the % HNA cells (i.e. 20 minute mark). The phenotypic diversity index indicated three disturbances (i.e., at the 20 minute, 50 minute and 60 minute marks, **Figure 4C**), of which the one at the 50 minute mark was more difficult to distinguish with the conventional metrics. Finally the robust clustering of the phenotypic fingerprints detected a total of five distinct community types (**Figure 4D**), which in combination with the community transitions detected by the cell density, %HNA cells, and phenotypic diversity index metrics allowed us to distinguish all six freshwater community contaminations. Because a conservative and robust clustering approach was used, the groundwater microbial community (i.e. contamination 2), despite invoking

the largest change in TCC and a moderate decrease in % HNA cells, clustered together with the drinking water microbial community into a single community type. If conventional k-medoids clustering with knowledge concerning the number of expected community types was used (i.e. k = 6), all six freshwater communities could be identified, yet the number of false positive cluster allocations increased (**Figure S5**).

The phenotypic features that underlie the differences between community types were further investigated. We visualized the contrasts between the average phenotypic fingerprints of the two primary fluorescence parameters of the contaminated community types and the baseline drinking water microbial community (**Figure 5**). This allowed us to identify specific populations in the flow cytometric data that became enriched or reduced in relative abundance during each contamination event (**Figure 5A**). Each contamination event caused an enrichment in relatively high nucleic acid content populations that were largely unique to each contamination. However, there were also distinct high nucleic acid populations for the pond and river water contaminations that were reduced in relative abundance. Overall, for each contamination there were regions in the phenotypic fingerprint that were either contamination-specific or shared with other contaminations that allowed for discriminating between the different microbial community disturbances (**Figure 5B**).

4. Discussion

Our goal was the quantification and characterization of microbial disturbances in aquatic microbial communities through the integration of real-time FCM and advanced fingerprinting analysis. We demonstrated that with this approach steady state conditions, gradual changes and sudden events, with disturbances from both axenic cultures and natural microbial communities could be detected and accurately quantified at high temporal resolution (**Figures 3**-**5**).

4.1. Monitoring disturbance events through advanced fingerprinting

In order to resolve all microbial contamination events the combination of at least two FCM fingerprint metrics (i.e. phenotypic diversity index and community type) and one quantitative descriptor (total cell

concentration or %HNA cells) was necessary. Each of these statistics provides a unique insight into the community structure of the microbial community. The phenotypic diversity index has previously been shown to strongly correlate with the taxonomic diversity of the microbial community of a cooling water system as well as natural lake bacterioplankton communities (Props et al. 2016a, Props et al. 2018). Therefore, the phenotypic diversity index may be able to serve as a proxy for shifts in the microbial community diversity of other engineered systems as well. Our observations during the spiking of axenic contaminants are consistent with these previous data; the phenotypic diversity rapidly declined indicating a reduction in the evenness component of the microbial diversity, i.e. a single taxon suddenly became highly abundant (**Figure 3**). The difference in phenotypic diversity index of the microbial community during the two strain contaminations can be explained by two factors: (i) the slight difference in strain concentration resulted in a less diverse community during the *E. coli* contamination events when compared to *P. stutzeri*, and (ii) the intrinsic phenotypic differences between the two strains led to distinct changes in the community phenotypic fingerprint (see (Buysschaert et al. 2018) for an example of strain-level differences in phenotypic fingerprints). As such, the sensitivity to detect single strain contaminations will be conditional on the nature of the contamination (e.g. phylogeny, physiology).

The diversity dynamics for the disturbances with indigenous microbial communities were less distinct as these natural communities typically possess diversities that are within the same range as that of the receiving community. In addition, natural freshwater communities, such as those used in this study, often differ in their phenotypic properties such as nucleic acid content and cell morphology, as measured through flow cytometry (Bouvier et al. 2007). These differing phenotypic properties have been associated with distinct phylogenetic groups (Proctor et al. 2018, Wang et al. 2009), but also variable functionality (i.e., more productive systems have higher HNA cell density) (Bowman et al. 2017, Servais et al. 2003). Most contaminations resulted in a relative enrichment of various HNA populations, which are typically composed of larger cells, with a high cell-specific activity and larger genome size (Servais et al. 2003, Lebaron et al. 2002). Contaminations or disturbances in LNA populations, such as those dominating the groundwater community (> 70%), may prove

316 to be more difficult to detect based on flow cytometric fingerprinting and will require further research.
317 However, our successful detection of a high LNA-content river water community in the tap water system
318 suggests that this is possible for certain contaminations with the current computational workflow.
319
320 Monitoring microbial diversity is important as it may potentially regulate a multitude of biological phenomena
321 such as invasion (De Roy et al. 2013) and community functionality (Servais et al. 2003, Wittebolle et al. 2009),
322 and as such deserves substantial consideration in engineered aquatic systems where outgrowths of pathogens
323 (Proctor et al. 2017, Chiao et al. 2014), biofilms (Proctor et al. 2016) or bio-corroding communities
324 (Choudhury et al. 2012, Chien et al. 2012) may occur. Phenotypic community types were defined by robust
325 clustering of the fingerprints of 60 s bins. This approach allowed us to clearly demarcate the transitions
326 between successive disturbances as well as between different types of disturbances. Different community
327 types may reflect both significant changes in community structure (Rubbens et al. 2017) and in the
328 phenotypic characteristics of the community (Muller 2007, Koch et al. 2013b) as a response to a disturbance.
329 From a practical perspective this metric is attractive as it provides operators with a binary descriptor
330 (disturbance/no disturbance) of the complex underlying changes in the microbial community. As we were
331 able to attribute specific phenotypic populations to the discrete community types (**Figure 5**) we envision that
332 supervised computational methods (i.e. machine-learning) will be able to drastically improve the sensitivity by
333 which fingerprinting methods can automatically detect and distinguish between microbial contaminants in
334 microbial communities. Analogous to our clustering approach, these supervised methods could function on
335 the fingerprint as a whole and in this case classify samples as contaminated or not contaminated. On the
336 other hand the properties of single-cell contaminants could be learned by machine-learning models and
337 employed to classify and enumerate single-cells contaminants similarly to how Rubbens et al. (2017)
338 characterized synthetic microbial communities. However, for both applications (i.e. sample and single-cell
339 classification) a sufficiently large data collection should be available that contains samples or cells annotated
340 with the classification label of interest (e.g., contamination status or cell-type).
341

342 Total cell concentration has been the most applied FCM metric for monitoring disturbances in aquatic
343 microbial communities of engineered systems (Hammes and Egli 2010, Van Nevel et al. 2017). It is the
344 easiest parameter to assess and interpret disturbances by, but it lacks any resolving power when the
345 disturbance affects the community structure and not the cell density of the community, such as through
346 balanced growth and lysis or if the invading community (partially) displaces the indigenous microbial
347 community. An example of the latter phenomenon can be found in the first disturbance of the
348 autochthonous microbial community in the drinking water system (**Figure 4C/D**). This disturbance could
349 only be detected using the other metrics. However, the accuracy of these metrics was shown to be highly
350 dependent on the sample size (i.e. number of cells measured) and as such on the temporal resolution. The
351 search for an optimal sample size highlights the critical trade-off between high temporal resolution and
352 accuracy in the data analysis, which is a decision the researcher should make, demonstrate and justify on a
353 case-by-case basis. Similar to our experimental design, we advise to perform suitable control runs for new
354 applications in order to determine acceptable constraints on each FCM metric. In particular for our study, we
355 opted to constrain the coefficient of variation on the FCM metrics to 5 %, corresponding to a maximum
356 temporal resolution of 60 s for the drinking water and 10-30 s for the river water community. This resolution
357 would be well suited for numerous microbial processes in both laboratory scale experiments and full-scale
358 engineered systems that can transpire within minutes (Koch et al. 2014, Muller 2007). While previous work
359 using kinetic or real-time flow cytometry addressed this to some extent (Arnoldini et al. 2013), samples in
360 those studies were either not stained or were of a nature that staining did not interfere with the experiment
361 (e.g., studying the kinetics of dye penetration into bacterial cells). We recommend that our analysis guidelines
362 should also be taken into consideration during the advanced data analysis of any manual or online FCM data
363 of SYBR Green stained samples in order to avoid false-positive classification of disturbance events.
364
365 **4.2. Future applications of RT-FCM technology**
366 There exist numerous research applications for RT-FCM technology, such as detailed tracking of disinfection
367 kinetics with oxidants such as ozone or chlorine (von Gunten 2003, Benarde et al. 1967), growth (Props et al.

2016b) and/or stress responses (Arnoldini et al. 2012), cellular grazing by invasive species (Props et al. 2018, Denef et al. 2017) or lysis by bacteriophages (Weinbauer and Höfle 1998). The application of RT-FCM technology is not limited to laboratory-scale studies and several applications in environmental or engineered aquatic ecosystems can be considered. Real-time flow cytometry was recently used in a 5 hour study to successfully measure changes in the cell concentration of the effluent of a drinking water biofilter under fluctuating operational conditions, and as a tool to simulate the effects of emergency chlorine disinfection procedures (Besmer and Hammes 2016, Besmer et al. 2017). In this regard, measuring bacterial detachment and stabilization kinetics in building plumbing during the backwashing of biological filters (Dai et al. 2018) or throughout the operation of cooling water systems (Props et al. 2016b) are interesting research avenues. The current RT-FCM instrumentation is primarily powerful for studying (eco-)systems or laboratory experiments that display dynamic behavior of which the exact kinetics are of primary interest. RT-FCM would as such not be suitable as a long-term monitoring device since extended runs will result in substantial operational costs (e.g. consumption of stain, attrition of tubing, fouling). For long term baseline monitoring, the use of online or manual FCM is advised (Hammes et al. 2012, Abu-Absi et al. 2003).

Conclusions

- High-frequency RT-FCM data was integrated with advanced fingerprinting methods to describe temporal disturbances in a natural aquatic microbial community.
- We demonstrated that multiple conventional and advanced fingerprinting metrics are required for the detailed characterization of microbial disturbance events.
- We provide analysis guidelines that should be taken into consideration during the advanced data analysis of manual, online, and real-time FCM data.
- This technology represents a powerful tool for research applications in various (microbiological) research fields.

Acknowledgements

This work is a tribute to Hansueli Weilenmann, whose Eawag career of dedicated technical assistance through many years is warmly acknowledged and much appreciated. Additionally, the authors acknowledge technical support from Bradley Kratochvil. This work was supported through the Inter-University Attraction Pole (IUAP) "μ-manager" funded by the Belgian Science Policy (BELSPO, P7/25) and Eawag Discretionary Funding.

Figures

Figure 1. Schematic presentation of the real-time flow cytometry (RT-FCM) approach taken in this study. A prototype continuous-staining device links a conventional flow cytometer and an experimental environment, coupled with various fingerprinting methods for data analysis. The experimental environment was a continuous stirred reactor with possibilities for wash-in/wash-out operation and contaminant spiking. The prototype extracts samples continuously with peristaltic pumping at a rate of 0.3 mL min^{-1} and then stains these samples continuously in a mixing chamber with a fluorescent dye. From the mixing chamber the sample flows through an incubation loop at a controlled temperature (35 °C), after which the sample is delivered to a sampling port compatible with a commercially available flow cytometer.

Figure 2. Influence of temporal resolution (and consequently the number of events per bin) on the accuracy of FCM-derived microbial community metrics for the drinking water and river water microbial communities. **(A)** Coefficient of variation (CV) for the phenotypic diversity index calculated from data at various temporal resolutions vs. the number of cells measured. The black line represents an ordinary least squares regression fit. **(B)** Coefficient of variation (CV) for the total cell concentration (TCC) calculated from data at various temporal resolutions vs. the number of cells measured. The black line represents a locally weighted regression fit. The horizontal dotted lines indicate a CV-threshold of 5%, which is commonly considered to be a good target value for conventional FCM metrics.

Figure 3. Repeated spiking of two axenic cultures (*E. coli* and *P. stutzeri*) in a continuous reactor containing non-chlorinated drinking water. Each culture was spiked three consecutive times for one minute in a 50 mL reactor with a drinking water flow through rate of 100 mL min^{-1}. Colored arrows on panels indicate the time periods during which the contaminations could theoretically be detected. These time periods are lagging approximately 10 minutes behind the actual disturbance events as a result of the incubation loop in the RT-FCM setup. **(A)** Total cell concentration (TCC), **(B)** %HNA cells and **(C)** phenotypic diversity index resolved at one-minute intervals. Error bars on the phenotypic diversity index indicate bootstrap errors (n =

100). Color gradients for (A), (B) and (C) indicate relative deviation from the mean (calculated from the first 15 data points) expressed in units of standard deviation. **(D)** Phenotypic community type as identified by robust clustering of the phenotypic fingerprints, each community type is highlighted by a specific color. The representative community type for each sample was determined after 100 bootstraps. Representative community types supported by less than 90 of the 100 bootstrap runs are colorless and highlighted by the star icons.

Figure 4. Subsequent contamination of the continuous drinking water reactor by five mixed natural communities (i.e. respectively bottled mineral water (Evian), groundwater, 20-fold diluted pond water, 10-fold diluted river water (Chriesbach River), 20-fold diluted river water (Glatt River)). Colored arrows on panels indicate the time periods during which the contaminations could theoretically be detected. These time periods are lagging approximately 10 minutes behind the actual disturbance events as a result of the incubation loop in the RT-FCM setup. **(A)** Total cell concentration (TCC) **(B)** %HNA cells and **(C)** phenotypic diversity index resolved at one-minute intervals. Error bars on the phenotypic diversity index indicate bootstrap errors (n = 100). Color gradients for (B) and (C) indicate relative deviation from the mean (calculated from the first 15 data points) expressed in units of standard deviation. **(D)** Phenotypic community type as identified by robust clustering of the phenotypic fingerprints, each community type is highlighted by a specific color. The representative community type for each sample was determined after 100 bootstraps. Representative community types supported by less than 90 of the 100 bootstrap runs are colorless and highlighted by the star icons.

Figure 5. (A) contrasts between the average fingerprints of the control and the contaminations as identified by the phenotypic community typing (Figure 4D). High density differences indicate populations or regions in the flow cytometry data that are enriched (Δ Density > 0) or reduced (Δ Density < 0) during contamination relative to the baseline drinking water community. **(B)** Overlay of the contrasts of (A) highlighting both overlapping and distinct zones that respond to each contamination.

453

References

Verstraete, W., Wittelbolle, L., Heylen, K., Vanparys, B., de Vos, P., van de Wiele, T. and Boon, N. (2007) Microbial resource management: The road to go for environmental biotechnology. Engineering in Life Sciences 7(2), 117-126.

Koch, C., Harms, H. and Mueller, S. (2014) Dynamics in the microbial cytome - single cell analytics in natural systems. Current Opinion in Biotechnology 27, 134-141.

Lautenschlager, K., Boon, N., Wang, Y., Egli, T. and Hammes, F. (2010) Overnight stagnation of drinking water in household taps induces microbial growth and changes in community composition. Water Research 44(17), 4868-4877.

Props, R., Monsieurs, P., Mysara, M., Clement, L. and Boon, N. (2016a) Measuring the biodiversity of microbial communities by flow cytometry. Methods in Ecology and Evolution 7(11), 1376-1385.

Guenther, S., Koch, C., Huebschmann, T., Roeske, I., Mueller, R.A., Bley, T., Harms, H. and Mueller, S. (2012) Correlation of Community Dynamics and Process Parameters As a Tool for the Prediction of the Stability of Wastewater Treatment. Environmental Science & Technology 46(1), 84-92.

Besmer, M.D., Epting, J., Page, R.M., Sigrist, J.A., Huggenberger, P. and Hammes, F. (2016) Online flow cytometry reveals microbial dynamics influenced by concurrent natural and operational events in groundwater used for drinking water treatment. 6, 38462.

Zhang, Y., Oh, S. and Liu, W.-T. (2017) Impact of drinking water treatment and distribution on the microbiome continuum: an ecological disturbance's perspective. Environmental Microbiology 19(8), 3163-3174.

Besmer, M.D. and Hammes, F. (2016) Short-term microbial dynamics in a drinking water plant treating groundwater with occasional high microbial loads. Water Research 107(Supplement C), 11-18.

Props, R., Kerckhof, F.-M., Rubbens, P., De Vrieze, J., Hernandez Sanabria, E., Waegeman, W., Monsieurs, P., Hammes, F. and Boon, N. (2016b) Absolute quantification of microbial taxon abundances. ISME J.

Dubelaar, G.B.J., Gerritzen, P.L., Beeker, A.E.R., Jonker, R.R. and Tangen, K. (1999) Design and first results of CytoBuoy: A wireless flow cytometer for in situ analysis of marine and fresh waters. Cytometry 37(4), 247-254.

Dubelaar, G.B.J. and Gerritzen, P.L. (2000) CytoBuoy: a step forward towards using flow cytometry in operational oceanography. 2000 64(2), 11.

Besmer, M.D., Weissbrodt, D.G., Kratochvil, B.E., Sigrist, J.A., Weyland, M.S. and Hammes, F. (2014) The feasibility of automated online flow cytometry for in-situ monitoring of microbial dynamics in aquatic ecosystems. Frontiers in Microbiology 5.

Hammes, F., Broger, T., Weilenmann, H.-U., Vital, M., Helbing, J., Bosshart, U., Huber, P., Odermatt, R.P. and Sonnleitner, B. (2012) Development and laboratory-scale testing of a fully automated online flow cytometer for drinking water analysis. Cytometry Part A 81A(6), 508-516.

Abu-Absi, N.R., Zamamiri, A., Kacmar, J., Balogh, S.J. and Srienc, F. (2003) Automated flow cytometry for acquisition of time-dependent population data. Cytometry Part A 51A(2), 87-96.

Zhao, R., Natarajan, A. and Srienc, F. (1999) A flow injection flow cytometry system for on-line monitoring of bioreactors. Biotechnology and Bioengineering 62(5), 609-617.

Martin, J. and Swartzendruber, D. (1980) Time: a new parameter for kinetic measurements in flow cytometry. Science 207(4427), 199-201.

Nolan, J.P. and Sklar, L.A. (1998) The emergence of flow cytometry for sensitive, real-time measurements of molecular interactions. Nature Biotechnology 16, 633.

Arnoldini, M., Heck, T., Blanco-Fernandez, A. and Hammes, F. (2013) Monitoring of Dynamic Microbiological Processes Using Real-Time Flow Cytometry. Plos One 8(11).

Vines, A., McBean, G.J. and Blanco-Fernández, A. (2010) A flow-cytometric method for continuous measurement of intracellular Ca2+ concentration. Cytometry Part A 77A(11), 1091-1097.

Juan, G., Cavazzoni, M., Sáez, G.T. and O'Connor, J.-E. (1994) A fast kinetic method for assessing mitochondrial membrane potential in isolated hepatocytes with rhodamine 123 and flow cytometry. Cytometry 15(4), 335-342.

Besmer, M.D., Sigrist, J.A., Props, R., Buysschaert, B., Mao, G., Boon, N. and Hammes, F. (2017) Laboratory-Scale Simulation and Real-Time Tracking of a Microbial Contamination Event and Subsequent Shock-Chlorination in Drinking Water. Frontiers in Microbiology 8, 1900.

Shapiro, H.M. (1983) Multistation multiparameter flow cytometry: A critical review and rationale. Cytometry 3(4), 227-243.

Hammes, F. and Egli, T. (2010) Cytometric methods for measuring bacteria in water: advantages, pitfalls and applications. Analytical and Bioanalytical Chemistry 397(3), 1083-1095.

Muller, S. (2007) Modes of cytometric bacterial DNA pattern: a tool for pursuing growth. Cell Proliferation 40(5), 621-639.

Mueller, S. and Nebe-von-Caron, G. (2010) Functional single-cell analyses: flow cytometry and cell sorting of microbial populations and communities. Fems Microbiology Reviews 34(4), 554-587.

Berney, M., Vital, M., Huelshoff, I., Weilenmann, H.-U., Egli, T. and Hammes, F. (2008) Rapid, cultivation-independent assessment of microbial viability in drinking water. Water Research 42(14), 4010-4018.

Prest, E.I., Hammes, F., Kotzsch, S., van Loosdrecht, M.C.M. and Vrouwenvelder, J.S. (2013) Monitoring microbiological changes in drinking water systems using a fast and reproducible flow cytometric method. Water Research 47(19), 7131-7142.

Bouvier, T., del Giorgio, P.A. and Gasol, J.M. (2007) A comparative study of the cytometric characteristics of High and Low nucleic-acid bacterioplankton cells from different aquatic ecosystems. Environmental Microbiology 9(8), 2050-2066.

Li, W.K.W. (1997) Cytometric diversity in marine ultraphytoplankton. Limnology and Oceanography 42(5), 874-880.

Rubbens, P., Props, R., Boon, N. and Waegeman, W. (2017) Flow Cytometric Single-Cell Identification of Populations in Synthetic Bacterial Communities. Plos One 12(1).

527 Stepanauskas, R., Fergusson, E.A., Brown, J., Poulton, N.J., Tupper, B., Labonté, J.M., Becraft, E.D., Brown,
528 J.M., Pachiadaki, M.G., Povilaitis, T., Thompson, B.P., Mascena, C.J., Bellows, W.K. and Lubys, A. (2017)
529 Improved genome recovery and integrated cell-size analyses of individual uncultured microbial cells and viral
530 particles. Nature Communications 8(1), 84.

531 Props, R., Schmidt, M.L., Heyse, J., Vanderploeg, H.A., Boon, N. and Denef, V.J. (2018) Flow cytometric
532 monitoring of bacterioplankton phenotypic diversity predicts high population-specific feeding rates by
533 invasive dreissenid mussels. Environmental Microbiology 20(2), 521-534.

534 Koch, C., Fetzer, I., Harms, H. and Mueller, S. (2013a) CHIC - An automated approach for the detection of
535 dynamic variations in complex microbial communities. Cytometry Part A 83A(6), 561-567.

536 Koch, C. and Müller, S. (2017) Personalized microbiome dynamics – Cytometric fingerprints for routine
537 diagnostics. Molecular Aspects of Medicine.

538 Amalfitano, S., Fazi, S., Ejarque, E., Freixa, A., Romaní, A.M. and Butturini, A. Deconvolution model to
539 resolve cytometric microbial community patterns in flowing waters. Cytometry Part A, n/a-n/a.

540 Reynolds, A.P., Richards, G., de la Iglesia, B. and Rayward-Smith, V.J. (2006) Clustering Rules: A Comparison
541 of Partitioning and Hierarchical Clustering Algorithms. Journal of Mathematical Modelling and Algorithms
542 5(4), 475-504.

543 Rousseeuw, P.J. (1987) Silhouettes: A graphical aid to the interpretation and validation of cluster analysis.
544 Journal of Computational and Applied Mathematics 20(Supplement C), 53-65.

545 De Roy, K., Clement, L., Thas, O., Wang, Y. and Boon, N. (2012) Flow cytometry for fast microbial
546 community fingerprinting. Water Research 46(3), 907-919.

547 Proctor, C.R., Besmer, M.D., Langenegger, T., Beck, K., Walser, J.-C., Ackermann, M., Bürgmann, H. and
548 Hammes, F. (2018) Phylogenetic clustering of small low nucleic acid-content bacteria across diverse
549 freshwater ecosystems. The Isme Journal.

550 Buysschaert, B., Kerckhof, F.M., Vandamme, P., De Baets, B. and Boon, N. (2018) Flow cytometric
551 fingerprinting for microbial strain discrimination and physiological characterization. Cytometry A 93(2), 201-
552 212.

553 Wang, Y., Hammes, F., Boon, N., Chami, M. and Egli, T. (2009) Isolation and characterization of low nucleic
554 acid (LNA)-content bacteria. Isme Journal 3(8), 889-902.

555 Bowman, J.S., Amaral-Zettler, L.A., Rich, J.J., Luria, C.M. and Ducklow, H.W. (2017) Bacterial community
556 segmentation facilitates the prediction of ecosystem function along the coast of the western Antarctic
557 Peninsula. Isme Journal 11(6), 1460-1471.

558 Servais, P., Casamayor, E.O., Courties, C., Catala, P., Parthuisot, N. and Lebaron, P. (2003) Activity and
559 diversity of bacterial cells with high and low nucleic acid content. Aquatic Microbial Ecology 33(1), 41-51.

560 Lebaron, P., Servais, P., Baudoux, A.C., Bourrain, M., Courties, C. and Parthuisot, N. (2002) Variations of
561 bacterial-specific activity with cell size and nucleic acid content assessed by flow cytometry. Aquatic Microbial
562 Ecology 28(2), 131-140.

De Roy, K., Marzorati, M., Negroni, A., Thas, O., Balloi, A., Fava, F., Verstraete, W., Daffonchio, D. and Boon, N. (2013) Environmental conditions and community evenness determine the outcome of biological invasion. Nature Communications 4.

Wittebolle, L., Marzorati, M., Clement, L., Balloi, A., Daffonchio, D., Heylen, K., De Vos, P., Verstraete, W. and Boon, N. (2009) Initial community evenness favours functionality under selective stress. Nature 458(7238), 623-626.

Proctor, C.R., Dai, D., Edwards, M.A. and Pruden, A. (2017) Interactive effects of temperature, organic carbon, and pipe material on microbiota composition and Legionella pneumophila in hot water plumbing systems. Microbiome 5(1), 130.

Chiao, T.-H., Clancy, T.M., Pinto, A., Xi, C. and Raskin, L. (2014) Differential Resistance of Drinking Water Bacterial Populations to Monochloramine Disinfection. Environmental Science & Technology 48(7), 4038-4047.

Proctor, C.R., Gachter, M., Kotzsch, S., Rolli, F., Sigrist, R., Walser, J.-C. and Hammes, F. (2016) Biofilms in shower hoses - choice of pipe material influences bacterial growth and communities. Environmental Science: Water Research & Technology 2(4), 670-682.

Choudhury, M.R., Hsieh, M.-K., Vidic, R.D. and Dzombak, D.A. (2012) Corrosion management in power plant cooling systems using tertiary-treated municipal wastewater as makeup water. Corrosion Science 61, 231-241.

Chien, S.H., Chowdhury, I., Hsieh, M.K., Li, H., Dzombak, D.A. and Vidic, R.D. (2012) Control of biological growth in recirculating cooling systems using treated secondary effluent as makeup water with monochloramine. Water Research 46(19), 6508-6518.

Koch, C., Fetzer, I., Schmidt, T., Harms, H. and Mueller, S. (2013b) Monitoring Functions in Managed Microbial Systems by Cytometric Bar Coding. Environmental Science & Technology 47(3), 1753-1760.

Van Nevel, S., Koetzsch, S., Proctor, C.R., Besmer, M.D., Prest, E.I., Vrouwenvelder, J.S., Knezev, A., Boon, N. and Hammes, F. (2017) Flow cytometric bacterial cell counts challenge conventional heterotrophic plate counts for routine microbiological drinking water monitoring. Water Research 113(Supplement C), 191-206.

von Gunten, U. (2003) Ozonation of drinking water: Part I. Oxidation kinetics and product formation. Water Research 37(7), 1443-1467.

Benarde, M.A., Snow, W.B., Olivieri, V.P. and Davidson, B. (1967) Kinetics and Mechanism of Bacterial Disinfection by Chlorine Dioxide. Applied Microbiology 15(2), 257-265.

Arnoldini, M., Mostowy, R., Bonhoeffer, S. and Ackermann, M. (2012) Evolution of Stress Response in the Face of Unreliable Environmental Signals. Plos Computational Biology 8(8).

Denef, V.J., Carrick, H.J., Cavaletto, J., Chiang, E., Johengen, T.H. and Vanderploeg, H.A. (2017) Lake Bacterial Assemblage Composition Is Sensitive to Biological Disturbance Caused by an Invasive Filter Feeder. Msphere 2(3).

Weinbauer, M.G. and Höfle, M.G. (1998) Significance of Viral Lysis and Flagellate Grazing as Factors Controlling Bacterioplankton Production in a Eutrophic Lake. Applied and Environmental Microbiology 64(2), 431-438.

601 Dai, D., Proctor, C.R., Williams, K., Edwards, M.A. and Pruden, A. (2018) Mediation of effects of
602 biofiltration on bacterial regrowth, Legionella pneumophila, and the microbial community structure under hot
603 water plumbing conditions. Environmental Science: Water Research & Technology.
604

Figure1

Click here to download high resolution image

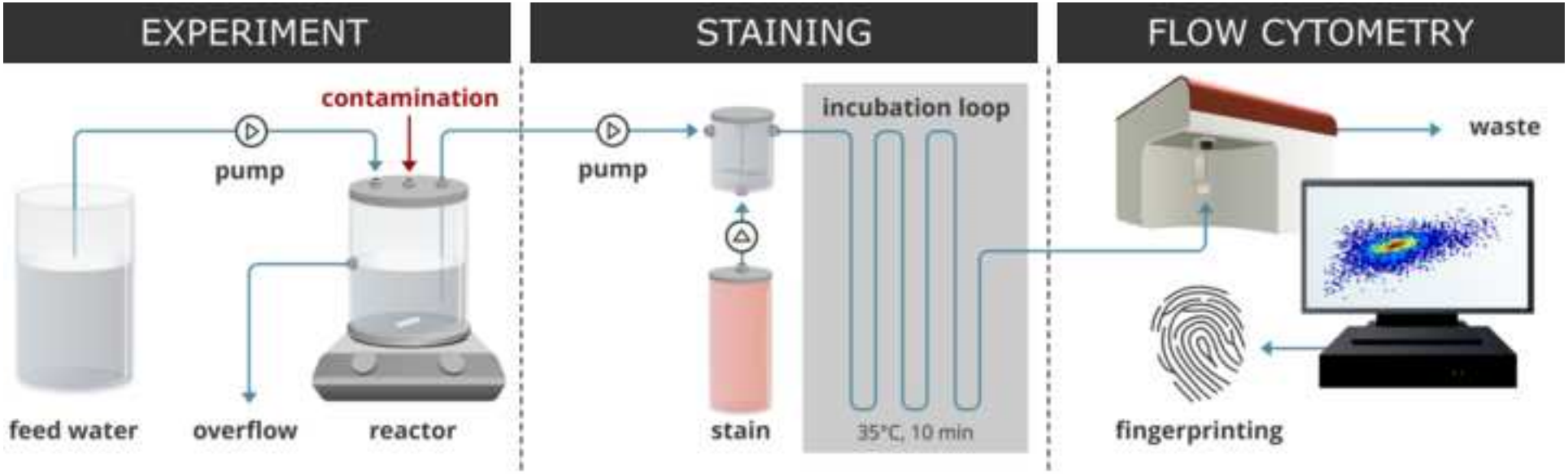

Figure2

Click here to download high resolution image

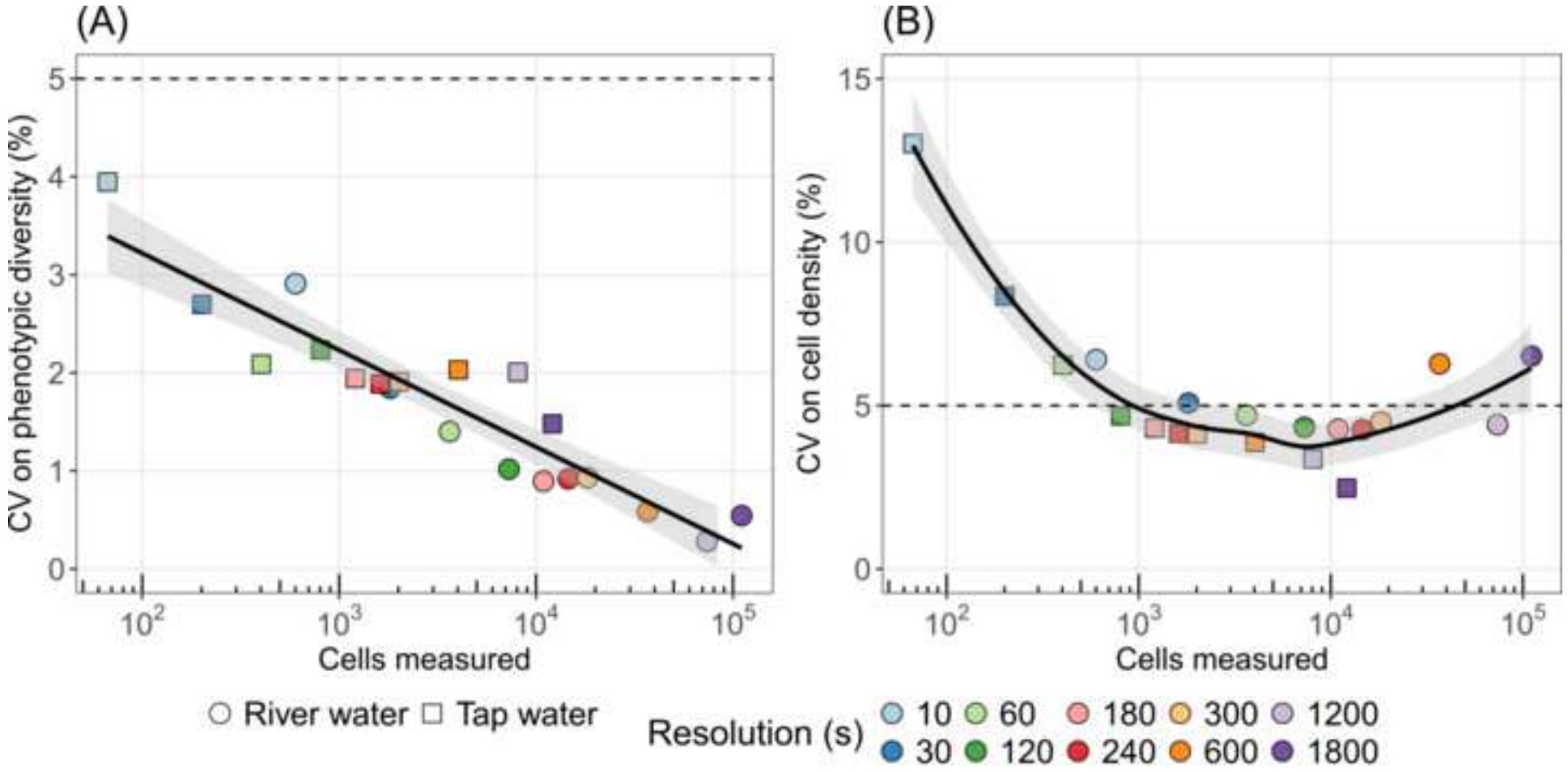

Figure3

Click here to download high resolution image

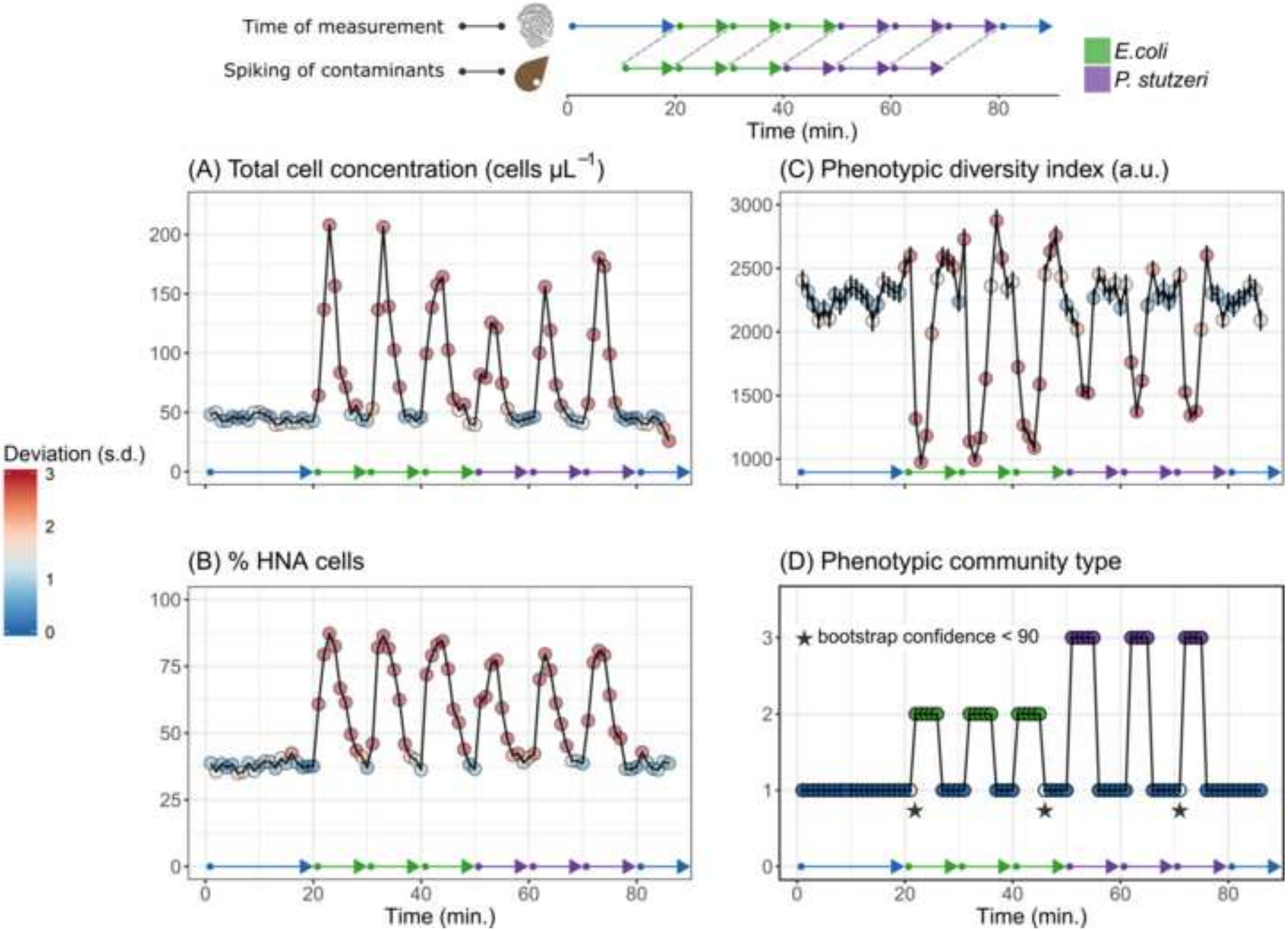

Figure4

Click here to download high resolution image

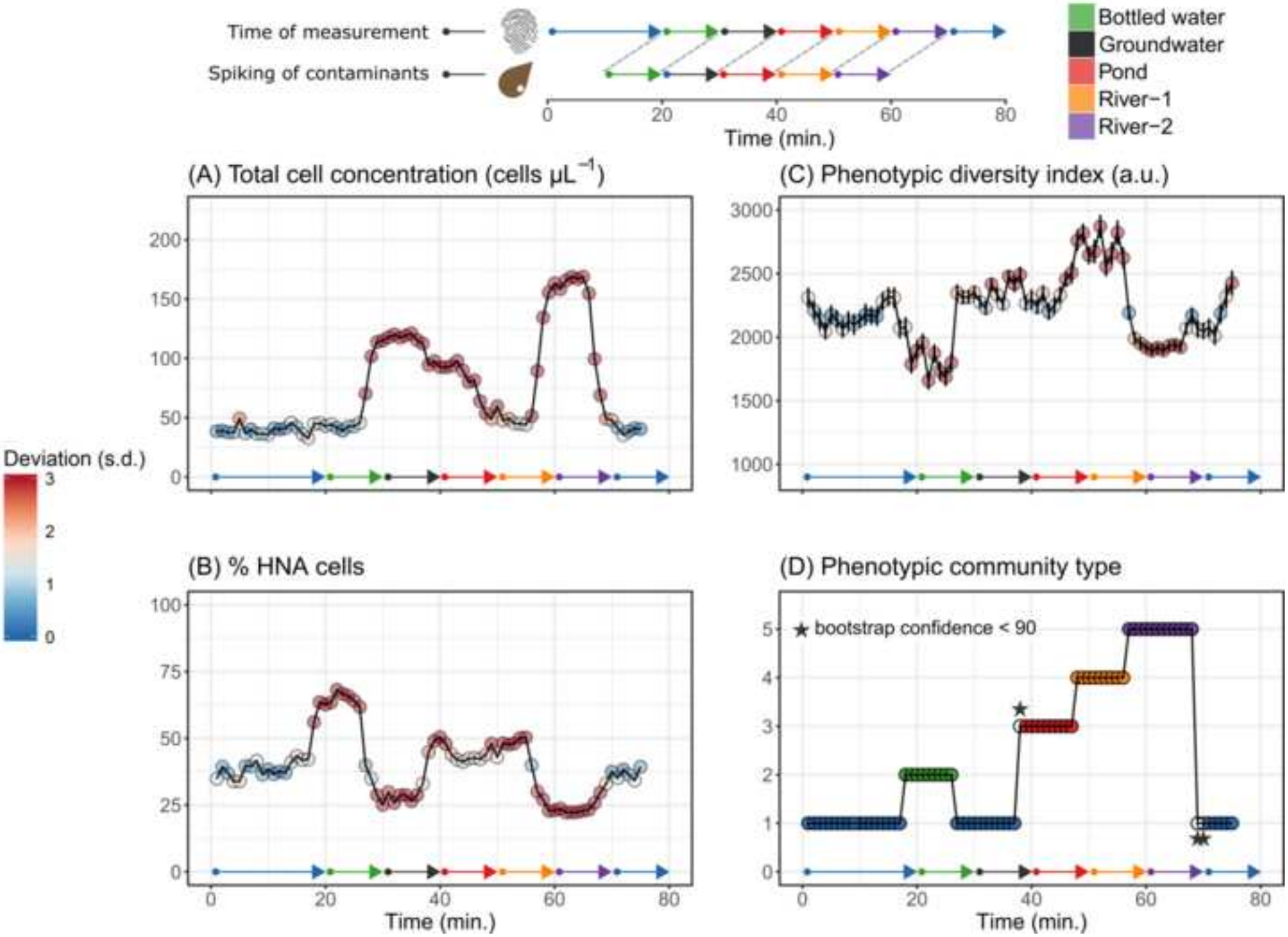

Figure5

Click here to download high resolution image